Supplementary Information

MXenes in healthcare: synthesis, fundamentals, and applications

Zaheer Ud Din Babar [a,b], Vincenzo Iannotti [c,d], Giulio Rosati [a], Ayesha Zaheer [c], Raffaele Velotta [c], Bartolomeo Della Ventura [c], Ruslán Alvarez-Diduk [a*], Arben Merkoçi [a,e*]

[a] *Catalan Institute of Nanoscience and Nanotechnology (ICN2), CSIC and BIST, Campus UAB, 08193 Bellaterra, Barcelona, Spain.*
[b] *Scuola Superiore Meridionale (SSM), University of Naples Federico II, Largo S. Marcellino, 10, 80138, Italy.*
[c] *Department of Physics "E. Pancini", University of Naples Federico II, Via Cintia 26, 80126, Naples, Italy.*
[d] *Institute for Superconductors, Oxides and other Innovative Materials and Devices of the National Research Council (CNR-SPIN), Piazzale V. Tecchio 80, 80125, Naples, Italy.*
[e] *ICREA Institució Catalana de Recerca i Estudis Avançats, Barcelona, Spain.*

* Corresponding authors
ruslan.alvarez@icn2.cat
arben.merkoci@icn2.cat

Supplementary Information - I

Quick check to access MXene synthesis in lab
Flake Size distribution and influencing factors
MXene Films and drying conditions
Oxidation and Restoring Oxidized MXene
Surface Chemistry of MXenes
Solution Processing and Printing

1. Quick checks to assess the synthesis of MXenes

You can check the success of MXene synthesis before performing sophisticated characterization. Typically, optical methods are straightforward. This can be achieved by dissolving a small amount of delaminated MXene in DI water and comparing the color of the suspension with that shown in **Fig. S1a**. Because MXenes exhibit a broad chromatic range, and their colloidal solutions display varying colors depending on their composition. The corresponding vacuum-filtered free-standing films or spray-coated films show complementary hues and varying optical responses (**Fig. S1b**). Thus, MXenes can be differentiated by their specific colours, particularly at low concentrations. At higher concentrations, it is challenging to observe well-defined transmission.

Another possible option is to record the UV-visible spectrum of the MXene colloids. Each MXene exhibits specific optical absorption (or transmission) peaks, and such extinction peaks not only change with varying "M" elements but also by changing "n", demonstrating the influence of both composition and structure on the observed optical properties (**Fig. S1c)**.

For size distribution, DLS measurements can be performed, as they provide an acceptable estimation of flake size [1]. With DLS, one can measure the zeta potential of MXene. However, it is important for such optical measurements to ensure that the MXene suspension is very diluted (translucent) and consistent, which means that there should not be particles or aggregates.

Conversely, for detailed structural analysis and to assess the quality of flakes, XRD and SEM (cross-sectional, in case of MXene films, and for top view, perform drop-casting of MXene suspension on Alumina Oxide substrate for better contrast). EDXs are usually coupled with SEM and can be used for elemental composition (useful to quantify the MAX to ml-MXene conversions). However, a detailed assessment of elemental composition techniques such as XPS or EELS is suggested [2].

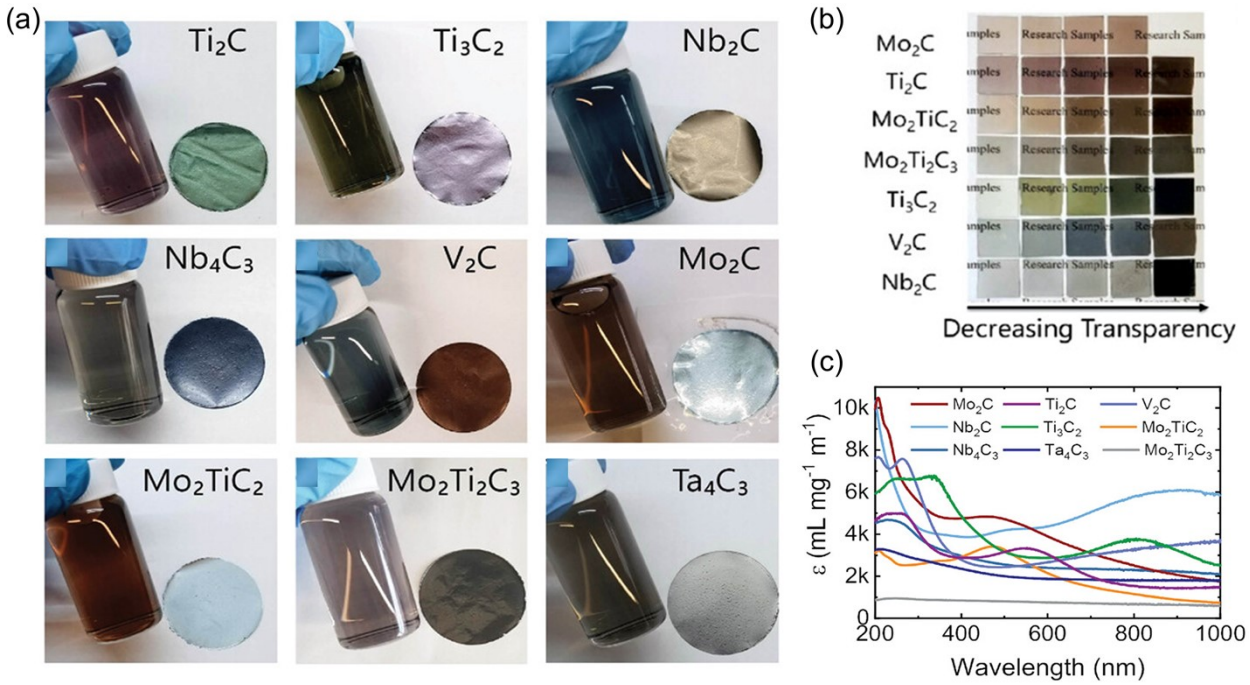

Fig. S1 (a) Digital photographs of the MXene suspension and corresponding films prepared by vacuum filtration, demonstrating the distinctive colour of each MXene. Colour transition of thin films of different thicknesses prepared by spray coating of as-produced MXene suspensions (varying optical density). UV-vis spectra at different wavelengths show distinctive extinction peaks for each MXene. *Reused after Permission from Ref. [3] © 2020 Wiley-VCH GmbH.*

2. Determining the flake size and associated factors

The size distribution of MXenes produced by liquid-phase exfoliation can vary from sub-nanometre to micrometer. This feature is particularly important when size-dependent applications are investigated [1]. In addition, flake dimensions also have a significant impact on the rheological behaviour (for printing, etc.) and electrical properties of MXene [4]. For example, the interflake contacts are greatly affected by the flake size and effectively determine the conductivity, mechanical and thermal properties. Studies have shown that MXenes with larger layer sizes show improved interflake contacts and better alignment in vacuum-filtered films and assembled fibres, ultimately leading to higher conductivity [5,6]. Factors such as the MAX particle size, etching conditions (e.g. etching route, etchant concentrations and parameters), and post-processing (e.g. sonication, handshaking, or soft delamination) can all be used to regulate the average size and quality of MXene flakes. Furthermore, sonication, which is frequently employed to increase delamination yield, can break large flakes into smaller ones. However, the safety precautions to be taken during sonication will be the same as those outlined above.

In the following section, we explicitly highlight the effect of several parameters on the size distribution of MXenes. We emphasize that these features and adjustments are application-specific, as the requirements for one application can differ significantly from the other.

2.1. Effect of MAX phase size: The grain size of the precursor MAX phase sets the maximum size restriction for MXene sheets. Zhang et al. demonstrated this aspect, reporting an improvement in the mechanical characteristics and electrical conductivity of the developed films [7]. Large MAX phase particles (10 ± 2.1 μm) were isolated from smaller ones by centrifugation. Consequently, etching conditions were adjusted accordingly, as we know that MAX phase size significantly alters the etching parameters. MXene films produced from such flakes using a scalable blade coating method exhibited notable properties: a tensile strength of ~570 MPa, a Young's modulus of ~20.6 GPa, and electrical conductivity of ~15,100 S cm^{-1}. Therefore, larger MAX-phase crystals should be synthesised to obtain sheets with larger lateral diameters, resulting in mechanically robust films with better conductivity.

2.2. Effect of etchant concentration: MXenes can be etched using various techniques, with each strategy affecting the flake size differently. Single- or few-layer flakes may be formed via sonicated HF-etched MXene powders; however, pre-/post-intercalation is essential for large-scale delamination. Alhabeb et al. analytically investigated the effects of the etchant concentration and choice of intercalating agents on the size, quality, and conductivity of flakes [8]. For example, the LiF (5M)/HCl(6 M) technique causes delamination by dramatically increasing the c-LP of $Ti_3C_2T_x$ through simultaneous intercalation of hydrated Li^+ ions between the layers. The product of this method is a sediment that behaves like clay, which can be sonicated to generate highly concentrated dispersions of the delaminated flakes in water. In contrast, defects are often introduced, and the size distribution can be significantly different from that of non-sonicated MXenes. Therefore, the etchant nature and concentration determine the use of sonication. On the other hand, increasing the molar ratio of LiF (from 5 to 7.5M) and HCl (from 6 to 9M) results in large flakes without requiring sonication. The term "minimally intensive layer delamination" (MILD) was introduced to highlight this gentler approach to produce larger single flakes, distinguishing it from the clay method. Furthermore, an optimised MILD method was introduced at a higher LiF ratio (12M) to synthesise MXene at room temperature, with significant swelling reported during the washing cycles. This signifies that apart from HCl, there is a threshold of Li^+ ions to initiate significant swelling so that large flakes can be separated without applying any mechanical shearing, thus preserving the quality.

2.3. Effect of delamination approach and centrifugation: Typical delamination can be size-limiting in MXene synthesis, particularly the approaches like sonication, vigorous hand, or vortex shaking. However, gentle hand shaking in a controlled manner, or a paint shaker is useful for increasing yield. Shekhirev et al. described a soft delamination method that allows the flakes to remain intact yet detach from the multilayer particles [9]. This provides another degree of freedom to tune the flake size independently of the MAX phase. In addition, Kanit et al. presented another crucial method through systematic investigations of $Ti_3C_2T_x$ size selection using statistical atomic force microscopy and electron microscopy [10]. Density gradient ultracentrifugation separates nanomaterials by size and thickness by employing variations in the sedimentation rates. This technique also shows potential for sorting and controlling the lateral size of MXenes [1]. Sedimentation-based separation (SBS) and liquid cascade centrifugation (LCC) techniques were also employed to segregate MXene flakes. Even after sorting at low centrifugal speeds of 2000 and 4000 rpm for 15 min using the SBS and LCC techniques, respectively, the flakes were primarily monolayers, and LCC provided higher yields and larger flakes. MXene flakes with an average length of 4.19 to 1.35 and 5.05 to 0.24 μm were found in solutions using LCC and SBS methods, respectively, at

higher speeds (from 3000 to 8000 rpm). This demonstrates the impact of the centrifugation technique, which aids MXene size selection.

3. MXene films and processing conditions.

Vacuum-assisted filtering (VAF) is frequently used to obtain MXene films of micrometer thickness. This technique requires a stable colloidal solution of MXene and produce films of individual nanosheets stacked in a compact structure, exhibiting exceptional flexibility. In this method, the concentration of MXene dispersion, flake size, and filtrate volume play important roles in determining the thickness, which ultimately determine the drying conditions, mechanical robustness, conductivity and electrochemical behaviour. Other parameters include the vacuum pressure, surfactant type, and filtration membrane type. The benefit of this approach lies in its simplicity and ability to fabricate hybrid MXene films by filtering the mixtures of MXenes and other materials [11]. These films enable sophisticated patterns in the required architectures and show potential for use in supercapacitors, EMI shielding, and flexible sensors [12].

The drying conditions of MXene films are critical as moisture can cause oxidation, which deteriorates the film's properties. High-temperature drying can remove interlayer water, thereby improving environmental stability and conductivity. Yury et al. reported that MXene films produced via VAF can retain nearly all their conductivity even after years of storage if vacuum-dried. Drying MXenes at 200 °C and above is a quick and effective way to boost their stability [13].

Synthesis processes also affect the MXene structure and, consequently, its stability. Bulky intercalants with large interlayer gaps, allow easier access to oxygen and water which can cause film deterioration. Short interlayer spacing can help prevent oxidation and degradation by excluding air and water, thus ensuring its stability over time. An important finding is that the conductivity of aged films can be restored by drying [13], this suggests that moisture between the MXene layers can be the primary cause of the observed decrease in conductivity, rather than structural deterioration, such as TiO_2 formation, which is irreparable.

4. Oxidation of MXenes and quick assessment techniques

Transition metals in MXenes, exist in a low-valence state, making them sensitive to oxidation, particularly in aqueous environments. This oxidation alters the fundamental characteristics of MXenes, posing significant concerns regarding their long-term shelf life. The oxidation process of flakes follows kinetic behaviour in aqueous environments and substantial experimental efforts has been devoted to understanding and mitigating this issue [14]. The composition of the MAX phase, synthesis procedure, preferred form (e.g., powder, film, ink), lateral size of the flakes, and storage conditions (type of solvent, concentration of colloidal solution, pH, and temperature) strongly influence MXene degradation [15,16]. Hydroxyl (−OH) and oxygen (−O) terminations on flake surface tend to attain a stable state and facilitate oxidation in the presence of surrounding water molecules or moisture. The oxidation often begins at the flake edges, leading to the formation of metal hydroxides or oxides, while the surface vacancies and defects accelerate this deterioration [17]. For instance, prolonged contact of $Ti_3C_2T_x$ MXene with water can cause its flakes to hydrolyse, as the oxygen in the water and air helps the formation of titanium dioxide (TiO_2). Doo et al., studied the oxidation mechanism of $Ti_3C_2T_x$ MXene in water media [18]. The −OH site were found particularly vulnerable where oxidation begins (**Fig. S2**). Moreover, oxidation process in

aqueous dispersions was found to be acidic driven as the oxidation enhances with pH. Under acidic conditions, protonated −OH groups on flakes increase the electrophilicity of Ti atoms, making them more prone to oxidative nucleophilic reactions with surrounding oxygen or water.

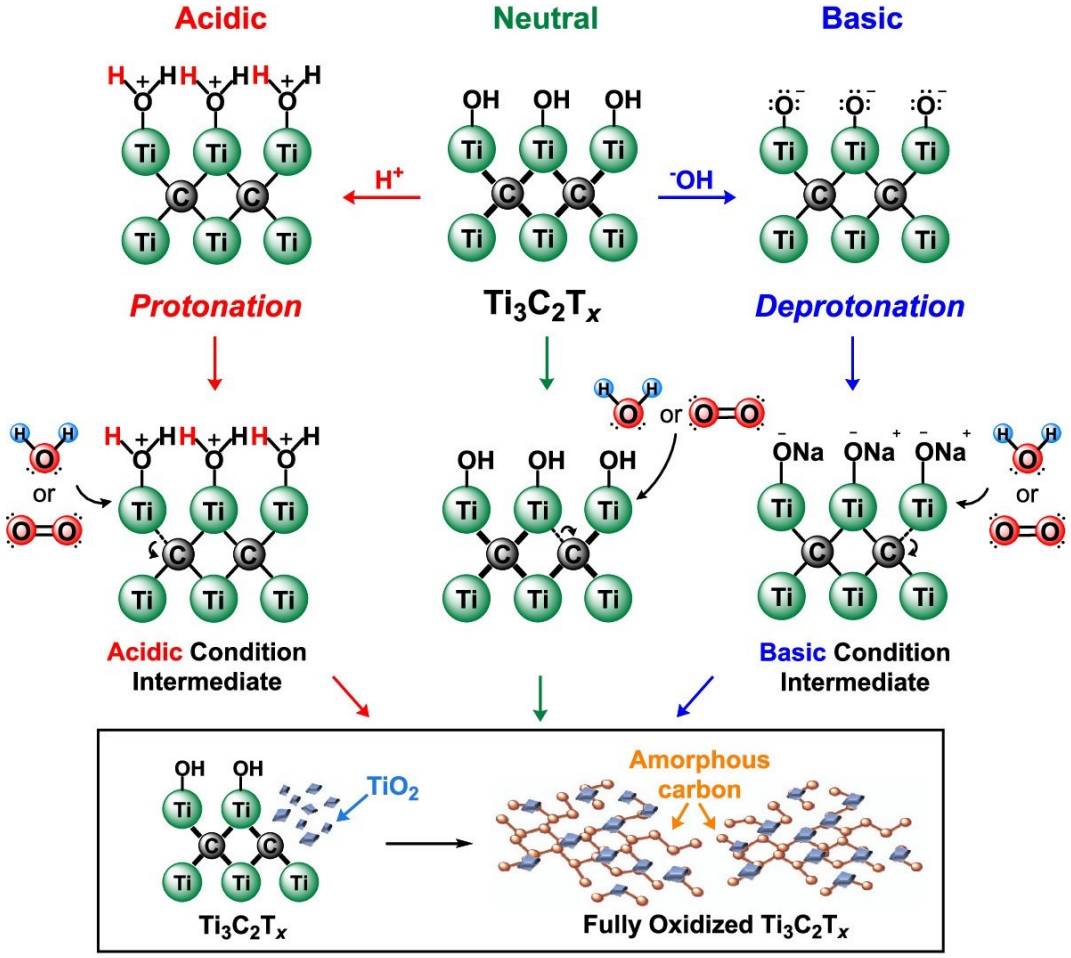

Fig. S2 Proposed oxidation mechanism of $Ti_3C_2T_x$ MXene in aqueous environments under different pH conditions. *Reused after Permission from Ref.[18], Copyright © 2021, American Chemical Society*.

Appropriate for first-hand observations, changes in the colour of MXene dispersions to lime white is the easiest way to verify oxidation. Other investigations suggest that conductivity measurements are the most reliable method for monitoring MXene oxidation [19]. However, from a laboratory perspective, colour changes and loss of colloidal stability can be considered the signs of oxidation. Another straightforward technique to quantitatively follow oxidation is UV–Vis spectroscopy of MXene suspensions [20]. This approach can provide valuable information regarding the time constant and is suitable for low concentrations. Since oxidation involves the formation of edge-formed metal oxide particles, which gives rise to different absorptions of incident light. The variation in the absorption peak can be related to the oxidation kinetics. Ti_3C_2 MXene, e.g., the intensity of absorption peaks at ~780 nm drops significantly upon oxidation and the TiO_2-representative band at ~237 nm also decayed exponentially.

There are numerous methods to overcome MXene oxidation, and the main ones are summarised here.

i) According to recent reports, a MAX phase with a more stoichiometric Al ratio results in shelf-stable MXene. The oxygen concentration of the MAX phases was significantly reduced in the resulting MXenes. However, this has only been documented for Ti_3C_2 MXenes [21].

ii) Oxidation and hydrolysis can be reduced if MXene is synthesised using a method that yields MXene flakes of a larger size with fewer defects [22,23].

iii) Another method to enhance the stability of MXenes, particularly M_2CT_x counterparts, is the intercalation of suitable molecules with controlled interlayer distances and composite formation [24,25].

iv) The oxidation rate can be reduced by removing the dissolved oxygen from MXene suspension via purging Ar gas and storing it at a low temperature; however, the flakes would still gradually deteriorate over time. It is also important to fill the storage vials up to full so that there is practically no space for air to be trapped inside the vial [17].

v) Vacuum filtration can remove water and produce films whose quality is unaffected by time or environment. The films have a longer lifespan (a decade) because of their compact architecture, preventing to interact with air [13]. Moreover, such films (referring only to pure films) can again be dispersed to create a colloidal solution by simply shaking or stirring in water or sonication for a shorter period.

vi) Another method for solving this issue is ion exchange and/or flocculation, preferable for extremely unstable MXenes such as V_2C [26]. Additionally, flocculation can help overcome the self-restacking or aggregation of MXene [27].

Nonetheless, there are numerous alternative approaches have been comprehensively compiled in literature to alleviate oxidation problem [22]. Interestingly, oxidation can be beneficial for specific applications. For instance, oxidized MXenes can enhance gas-sensing performance and serve as scavengers of reactive oxygen species (ROS) in targeted therapeutic interventions [28,29].

4.1. Restoring Oxidized MXenes

Oxidation of MXene is inevitable in typical environmental settings. In particular, the ability to re-use oxidised MXene and poor flakes dispersion limits their translation into commercial reality. When kept in aqueous media, MXenes last only a few days to a few weeks before fully oxidising. Such a weak resistance to oxygen is inefficient from an economic and practical standpoint. As discussed in the previous section, several strategies have been proposed to increase the oxidation stability of MXenes. However, recycling the oxidised MXenes seem beneficial and ideally require a straightforward technique to restore their original features while preserving their structure. Removing oxidation and further ligation with the right chemical groups might offer a comprehensive solution to the issues listed above. Nguyen et al. treated oxidised $Ti_3C_2T_x$ MXene films with hydrofluoric acid (HF) to restore their deteriorated qualities and reported an increased stability. However, these acids tend to break down MXenes [30]. Moreover, oxide layers can also be removed by mechanical methods, such as subjecting MXenes to short (60 seconds) but high-frequency (10 MHz) nanometre-amplitude surface-localised electromechanical vibrations [31]. This allows their electrical and electrochemical performance to be recovered under ambient conditions without the need for chemical additives or reducing agents. According to XPS analysis, there was a reduction of ~61%. in the total oxide content. Simultaneously, the capacitive performance of the material recovered to a level similar to that of the pristine films before oxidation.

In short, restoring oxidized MXenes is crucial for their commercial viability. Current methods, both chemical and mechanical, show promise but come with their respective challenges. HF treatment can restore MXene properties but risks structural integrity, while mechanical methods preserve the structure but require further study. Future research should focus on refining these techniques and developing straightforward, cost-effective restoration methods will significantly enhance the practicality and economic feasibility of MXenes.

5. Surface Chemistry and Functionalization

Understanding and manipulating the surface chemistry of MXenes is crucial for exploring their novel functionalities. The etching and delamination routes of MXenes lead diverse microenvironments (–OH, –O, –Cl, or –F or -Cl terminations) (**Fig. S3a**). Such terminations significantly influence the chemistry of the flakes, profoundly affecting their stability and interactions with the surrounding environment. Acid etching of MXenes has limited control over terminations, and the surface predominantly exhibits more –F terminations than –O/–OH terminations (**Fig. S3b**). Furthermore, the density of the –F terminations could be further modulated by adjusting the acid concentration. In addition, the complete removal of –F terminations or replacement by –O/–OH terminations can be achieved by treating MXene with Molten salt routes [32] (**Fig. S3b**). Such routes permit halogen termination at the desired concentrations and yield uniform termination. Remarkably, other terminations, such as –S, –Se, –Te, –P, and –Sb, can be uniformly applied to MXene (**Fig. S3b**). The molten-salt method facilitates the synthesis of –Cl or –Br terminated MXenes (for example, $Ti_3C_2Cl_2$, $Ti_3C_2Br_2$, and Nb_2CBr_2), which can serve as templates for post-synthetic MXenes terminated with –S, –Se, –Te, –NH, and –O, as well as bare or –H-terminated MXenes [33]. Uniform –O and –C terminations can be achieved by thermally treating MXene in different gases. For instance, heating MAX phases in an HCl atmosphere resulted in Cl-terminated MXene, and similarly, −S, −Se, −Te, and −P terminated MXene can also be realised with various gases (**Fig. S3c**) [34]. According to computational modelling, there are four possible sites where terminal groups can reside in $Ti_3C_2T_x$ (**Fig. S3c, left to right**). (i) Above and below the central Ti atoms in an FCC configuration. Theoretical and microscopic evaluations suggest that FCC is the most favourable location for termination [35]. (ii) "top" arrangement, where the termination occupies the top of the surface Ti atoms. (iii) A hexagonal close-packed (HCP) arrangement in which the terminal groups are directly positioned above the C atoms. (iv) Bridge configuration when termination resides between the Ti atoms but is not defined as either FCC or HCP.

X-ray photoelectron spectroscopy (XPS) and Nuclear Magnetic Resonance (NMR) are valuable tools for assessing MXene surfaces. Quantitative NMR experiments have highlighted a significant disparity in the abundance of –OH terminations compared to –F and –O terminations [36]. Raman spectroscopy can be used to survey MXene. Asia et al. reported a detailed Raman analysis of the effect of etching on the surface environment of $Ti_3C_2T_x$ MXenes [34]. In-plane (E_g) vibrations in Raman spectra within 230−470 cm^{-1} were defined as surface group regions. MXenes produced and subsequently processed by different routes (e.g. HF-MXene, HF−HCl MXene, Li^+ intercalated clay) show variations in the surface group region despite showing similar patterns. Variations in –O/–OH components lead to such differences in surface group region (**Fig. S3d**). In restacked films, this region is significantly evident compared to the others which can

be attributed to weak coupling among the flakes due to random orientation, subsequently strengthens the surface group vibrations (**Fig. S3e)**. Another important observation is the downshifting of the (out-of-plane vibrations) A_{1g}(Ti, C, T_x) peak with HF etching (730 – 738 cm^{-1}), which indicates intercalation-associated delamination, more interlayer opening, and a lower concentration of defects (**Fig. S3e)**. Variations in in-plane (E_g) and out-of-plane (A_{1g}) vibrations with different synthesis methods predominantly reflect the different behaviours of surface atoms, depicting versatile surface chemistry and therefore can be used as fingerprints for surface terminations. Certainly, terminations of MXenes are intriguing, and their dependence on various aspects signifies their importance in providing new characteristics and expanding their applications.

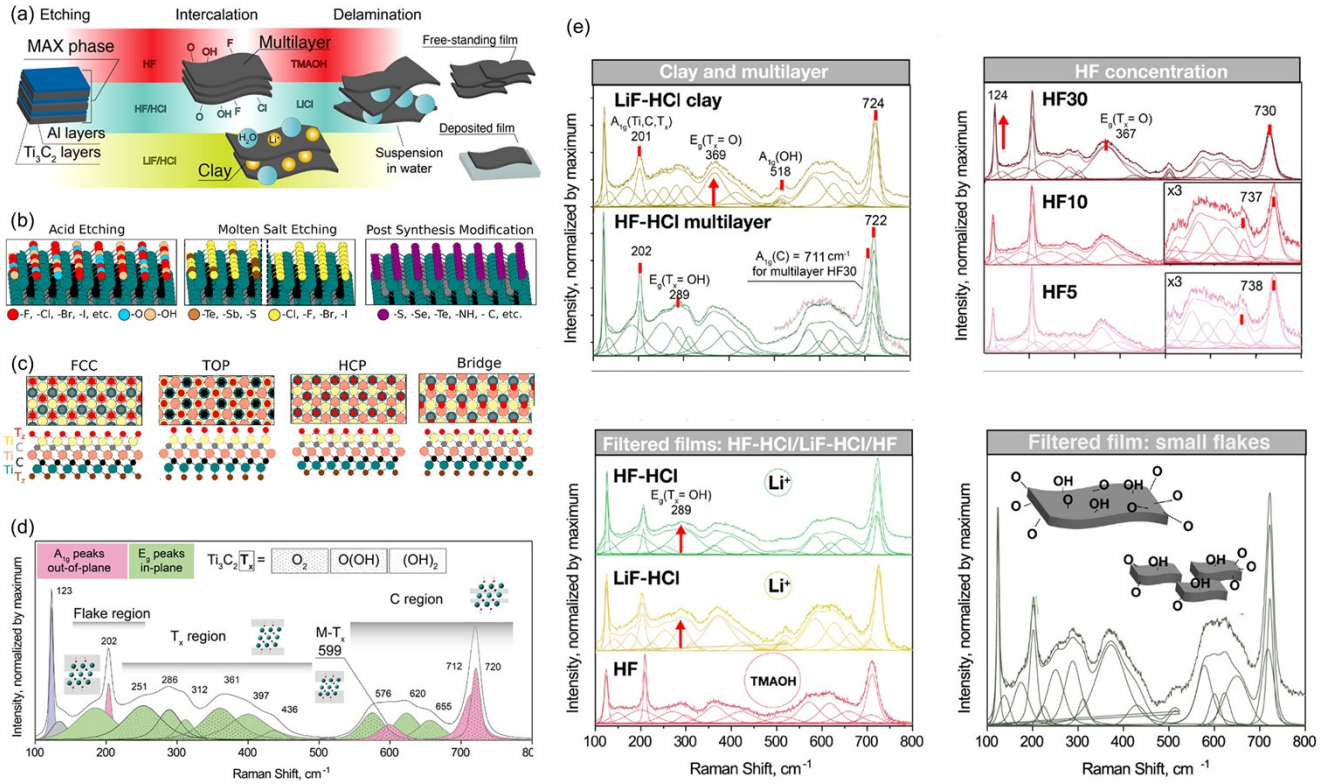

Fig. S3 (a) Different synthesis routes for $Ti_3C_2T_x$ MXene lead to different surface environments, and different delaminating agents for each etching route leave different ions over/within the MXene flakes. *Reused after Permission from Ref. [37] Copyright © 2020, American Chemical Society.* (b) Diversity of MXene surface groups as termination varies according to the etching method and subsequent treatments can lead to a single functional group. (c) Theoretically, functional groups can reside in four possible crystallographic configurations and are allocated to FCC, TOP, HCP, and bridge sites. *Reused with Permission from Ref. [35] Copyright © 2023, American Chemical Society.* (d) Various regions of Raman spectra of Ti3C2Tx MXene produced from HCl+HF method. (e) Raman spectra showing a comparison of multilayer samples produced by three different etching methods, different HF concentrations, and MXene films. *Reused after Permission from Ref. [37] Copyright © 2020, American Chemical Society.*

6. MXene processing and Printing

Functional inks, and controllable modification of MXenes allows their use in 3D printing, inkjet printing, and other printing techniques to fabricate sensing devices and biomedical prototypes [38]. As Constrained by a specific printing technique, nanofunctional inks obtained from 2D materials must satisfy several requirements **(Fig. S4a)**[4]. Also the modifications performed to achieve ink printability have also an effect on the print characteristics and post-printing treatments. Flake size, surface tension, ink solvent, viscosity, and additives used to avoid stacking and clustering of flakes are the main parameters to define the quality of an ink **(Fig. S4b)**. Hence changing one of the aforementioned parameters typically influences the other parameters. Particularly in inkjet printing, flake size plays a crucial role to prevent the clogging of printhead nozzles. It is recommended that the flake dimensions should be at least 100 times smaller than the nozzle diameter. Once a valid flake dimension is defined, it is important to analyse the colloidal stability of the dispersion, which is typically well-represented by zeta potential. MXenes are known to have good zeta potentials, typically in the range of -30 mV to -60 mV [39]. However, In cases of poor stability (chemical or colloidal), capping agents can be used to make it stable as commonly done with nanoparticle-based inks. The stability is also associated with the ink solvent—meanwhile, the choice of ink solvent is controlled by the rheological constraints of the printing technique. Water is the most commonly used solvent in inkjet printing. Also, the viscosity and surface tension must be precisely tuned to satisfy the requirements of the selected printing method. To achieve this, additives like water and several organic compounds, including DMSO, DMF, NMP, and ethanol are typically used [40]. An interesting possibility offered by MXenes, and recently investigated by many researchers, is the fabrication of additive-free inks. In fact, the flake dimensions and concentration of MXene strongly influence the rheology of its dispersion [39-42]. One of the most important problems associated with MXenes is their oxidative instability at room temperature and in aqueous solutions [43]. Even when the best printing conditions for a specific printing method are met and the MXene ink is printable and stable, this does not mean that the characteristics of the printed structures/devices meet the requirements of the targeted application. Conductivity, nanostructure/porosity, capacitance, electrochemical properties, and functionalization possibilities are among the desired characteristics of printed devices[4]. Conductivity differentiates not only the materials but also the nanostructured architectures at the nanometric level. The more conductive a material is, the more applicable it can be in electronics and bioelectronics. The nanostructure defines the surface-to-volume ratio of the printed material, and thus, its electrochemical activity and possible electrocatalytic properties. Capacitance is very important in general and for stacked materials, opening the way for supercapacitor applications[41]. Finally, the availability of functional groups on the flake surface is the key so that the devices can be easily functionalized with bioreceptors such as antibodies, enzymes, and DNA. Post-treatments are typically needed to cure and treat printed inks, and freeze-drying, curing, and annealing are just a few of the possible treatments, which most often are limited by the type of substrate (e.g. silicon, glass, plastic, paper, etc.). Each printing method requires a different post-treatment method and the type of post-treatment strongly influences the final properties of the printed film and device[38]. The main concept to be clear about this point is that the ink formulation, printing method, substrate, and post-treatments are not separated parts of the fabrication chain, but interconnected sides of the same. A change to any of them has a direct influence on all others, and this defines the final properties of the produced devices.

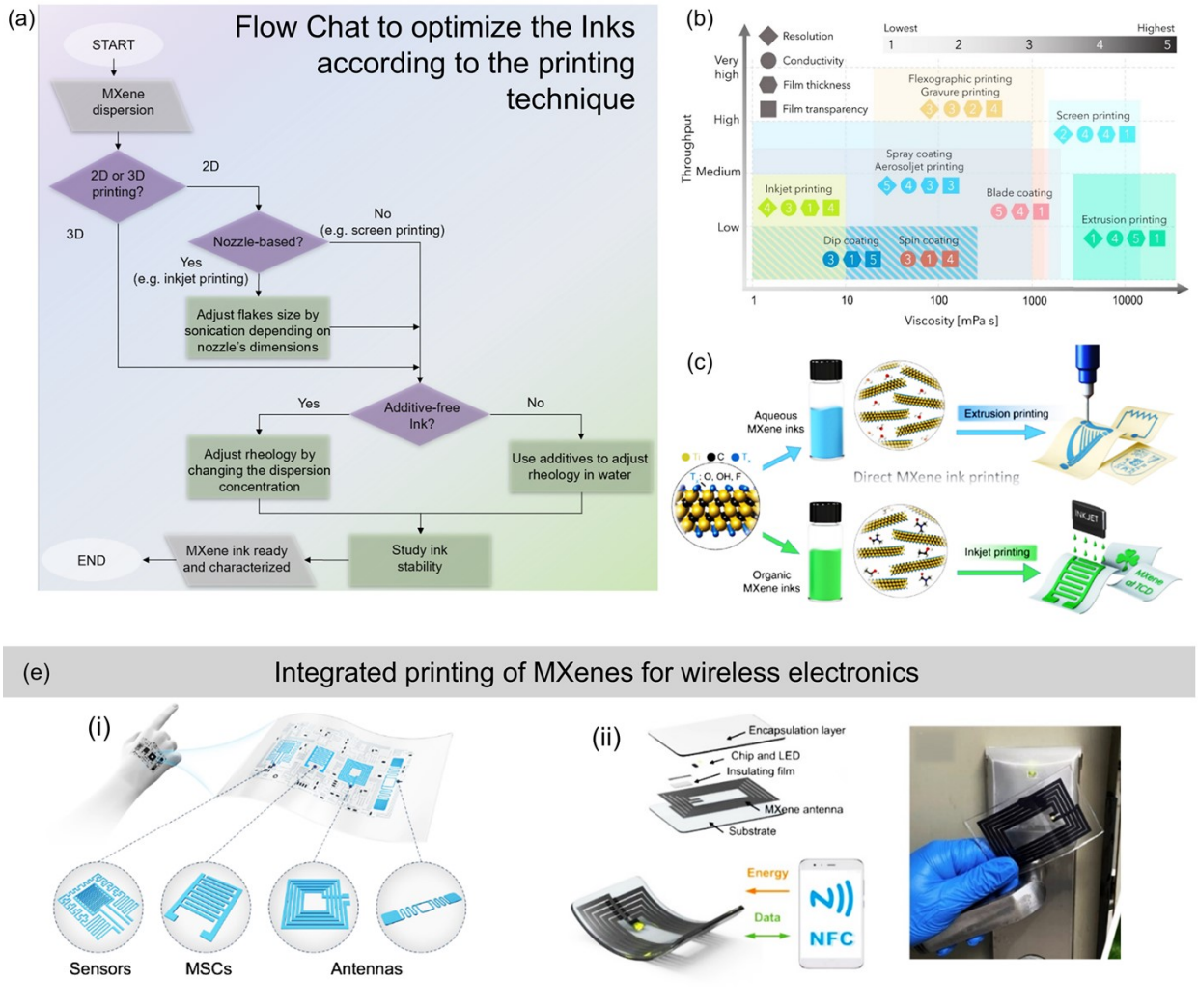

Fig. S4 (a) Process flowchart to prepare (or optimize) MXene inks as per the requirements of a printing technique. (b) A map interconnecting the solution processing of MXene colloids (viscosity vs. Throughput) across all important printing/coating methodologies and the their impact on physical features of printed design. *Reused after Permission from Ref.* [4] *© 2021 The Author(s). Published by Elsevier Ltd.* (c) Illustration of direct printing using aqueous $Ti_3C_2T_x$ ink and organic inks in ethanol (in bottom panel) for inkjet printing of diverse patterns. *Reused after Permission from Ref.* [44] *Copyright © 2019, The Author(s).* (d-i) Fabrication process and operational principle for direct printing of MXene-based NFC tags capable of wireless communication with smartphones and powering LED. (d-ii) MXene NFC tags serve as access cards for conventional electronic door locks. *Reused after Permission from Ref.* [45] *Copyright © 2022, The Author(s).*

For example, Quain et al. first demonstrated MXene printing on a thermal HP printer but was limited to a single pass on blank paper, making it incompatible with many micro- or nanofabrication procedures [46]. Zhang et al. extensively demonstrated MXene ink formulation and reported direct printing of additive-free, concentrated MXene inks, achieving high printing efficiency and spatial uniformity [44].In addition, organic $Ti_3C_2T_x$ inks have also been utilised for extrusion and inkjet printing **(Fig. S4c)**. Recently, extrusion-printable MXene aqueous inks have been reported for wireless electronics, such as MXene-printed NFC antennas [45]. **(Fig. S4d i, ii)**. This enables simultaneous wireless power harvesting, data

transmission with temperature and humidity sensing. Saleh et al. reported inkjet-printed $Ti_3C_2T_x$ MXene cutaneous electrodes for vital signs and electrophysiology monitoring under ambient conditions [47]. The fabricated patches also showed the possibility for sodium quantification in sweat and offer antibodies functionalization for pro-inflammatory cytokine proteins detection. Furthermore, MXenes are extremely attractive for supercapacitor development because of their inherent stacked structures, and several studies have focused on stamping, printing, and direct writing of MXene inks [41].. Nevertheless, MXene-based devices are on the rise and have great potential for use in electrochemical biosensing. Nevertheless, (stand-alone) fully printed electrochemical biosensors uniquely based on MXenes are still uncommon. Most often, MXenes are combined with other nanomaterials and simply drop casted on printed or commercial devices.

Supplementary Information - II

- **Biocompatibility, antimicrobial features and biodegradability**
- **Ecological Impact of MXenes**

8. Biocompatibility and ecological assessment of MXene

Biocompatibility and toxicity are two essential terms that are often used to assess the biosafety of any material. The term "biocompatibility" describes the compatibility of a substance with living tissues and its ability to function safely. Thus, biocompatibility includes the stability of a substance inside the body and the effect of its by-product during any biological transformations until removed from the body. Evaluating cytotoxicity is vital for biocompatibility assessments and for a material to be deemed biocompatible, it must demonstrate non-cytotoxic characteristics. MXenes toxicity is quite complicated and depends on many factors.

Synthesis: As the common routes for MXenes synthesis involves extremely corrosive acids, various metal ions, and organic/inorganic solvents for intercalation and delamination. If not washed away effectively, the presence of toxic ions (F^- and/or Li^+) can be harmful and induce cell apoptosis. The stability and aggregation of MXenes in physiological media are other factors that can pose health risks. In addition, by-products such as metal oxides can also be harmful. Specifically, V_2CT_x, which is believed to be the least stable of all experimentally synthesised MXenes, showed decreased cell viability upon oxidation. The decomposition of V_2CT_x into the extremely hazardous vanadium oxide is closely linked to its cytotoxicity [48]. Therefore, the primary objective should be to develop secure routes of MXene synthesis and overcoming the oxidative instability.

MAX and MXenes: Compared to MAX and *ml*-MXene, d-$Ti_3C_2T_x$ displayed more toxicity and significant antibacterial action. Ti_3AlC_2-MAX, *ml*-$Ti_3C_2T_x$, and d-$Ti_3C_2T_x$ MXene dispersions showed antibacterial activities against *E. coli* bacteria with 14.39%, 30.55%, and 96.70% reductions in cell viability, respectively [49]. Similarly, d-Nb_2CT_x and d-$Nb_4C_3T_x$ MXenes are more toxic (inhibiting bacterial growth) than their as-etched multilayered counterparts [50]. Additionally, toxicity also varies with "*n*" values; comparing d-Ti_2CT_x vs. d-$Ti_3C_2T_x$ and d-Nb_2CT_x vs. d-$Nb_4C_3T_x$, the latter of each more n-value showed higher toxicity to bacterial cells. The ability of individual sheets to function as "nanoknives" can be linked to the strong antibacterial qualities of their delaminated counterparts [50]. Furthermore, the isolated MXene flakes are anionic and bind to cationic sites on the cell membrane via direct physical contact,

thereby destroying the cell envelope (membrane rupture). The direct contact killing mechanism suggests MXenes can also promote bacterial contact with their surface, leading to the inactivation of attached microorganisms. Moreover, bacterial inhibition may arise from hydrogen bonding between the lipopolysaccharide sequences of the cell membrane and the oxygenated surface of MXenes [49].

Flake size: In addition to their morphology, the lateral size of MXene sheets also promotes cytotoxicity and allow over bactericidal properties. Studies have reported that cell viability decreases as the lateral size of sheets is reduced. Ti_3C_2 MXene nanosheets with 0.09 μm size showed higher toxicity (higher antibacterial activity) against B. subtilis and E. coli than large flakes (4.40 μm) [51]. Pandey et al. revealed size-dependent antimicrobial properties of Nb_2CT_x and $Nb_4C_3T_x$ MXenes against S. aureus and E. coli bacteria [50]. This increased activity at reduced lateral sizes can be quantitatively linked to the existence of excess sharp-edged nanoflakes which increase bacterial membrane rupture. Another plausible reason is that smaller nanosheets can easily enter cells via endocytosis by damaging the outer cell wall and cytoplasmic elements inside the cell [49]. However, it is also important to control the sheet size. This is because the sheets can transform to pseudospherical particles. In this case, the nanoknife effect is no longer effective, and the sheets become incapable of damaging bacterial membranes [50].

Concentration or Dose: Higher concentrations or dosages of MXene, which are beyond the capacity of cell recovery systems, result in increased toxicity. Note that the dose of a tested material is considered nontoxic if the cell viability loss is not more than 30% after 24 h of exposure. For example, $Ti_3C_2T_x$ at 200 μg mL^{-1} resulted in over 98% loss in cell viability of *B. subtilis* and *E. coli* compared to lower dosages [49]. Similarly, the d-Nb_2CT_x and d-$Nb_4C_3T_x$ MXenes exhibited a linear increase in toxicity as their concentrations increased [50]. One possible justification is that, as the amount of MXene increases, MXene sheets wrap or trap microorganisms and form aggregates that prevent bacterial growth. In addition, their strong reductive nature and reactive surfaces are responsible for such antibacterial properties [49,50]. At a lower dose of 12.5 mg mL^{-1}, $Ti_3C_2T_x$ showed no noticeable side effects on neural stem cells (NSCs) and NSC-derived differentiated cells. However, at higher doses (25 mg mL^{-1}), significant cytotoxicity and internalization into NSCs were observed, which significantly increased their apoptosis rate [52]

Effect of cell type: In-vitro toxicity also varies according to the target cell type. Ti_2NT_x showed strong toxicity in cancerous cells, almost twice that normal cell lines at higher concentrations [53]. Similarly, compared with normal cell lines (e.g. MRC-5 and HaCaT), $Ti_3C_2T_x$ was more toxic to cancerous cells (A549 and A375) [54]. Additionally, Scheibe et al. reported higher short-term cytotoxicity of $Ti_3C_2T_x$ in cancer-derived HeLa cells than normal human fibroblasts [55]. Similarly, Jastrzebska et al. highlighted the effect of thermal treatment and sonication on the oxidation of $Ti_3C_2T_x$ surface and employed MTT assays to evaluate cytotoxicity [56]. Oxidised-$Ti_3C_2T_x$ exhibited selective toxicity in malignant cell lines at concentrations upto 375 mg L^{-1}. This also indicates that oxidation has an important impact on toxicity, and it varies according to the cell line. Cancer cells generally have higher metabolic rates and greater oxidative stress than normal cells do. MXenes can generate reactive oxygen species (ROS) in the tumour microenvironment, which results in further oxidative damage to tumour cells and yields selective responses.

Reactive oxygen species (ROS) generation: MXenes produce ROS such as superoxide anion radical (O_2^-) and a hydroxyl radical (OH·) upon interacting with O_2 and H_2O, respectively. In addition, exposure to IR increases ROS formation. ROS damage bacterial cells through oxidative stress, causing membrane

disruption, DNA damage, interference with essential cellular functions, and ultimately, cell death [49,50]. Meanwhile, ROS generation and the cytotoxic behaviour of MXenes have been exploited for therapeutic use to destroy tumour cells. Owing to their synergistic combination of selective toxic effects and light-to-heat conversion capability, MXenes have been employed as photothermal therapy (PTT) agents in cancer treatment [57]. In addition to tumour cells, further research is needed to understand how other cell types, particularly those in pathological states, respond to MXenes.

In-vivo studies Prior to human testing, in-vivo studies are performed to assess the functionality and validate the impact of any nanomaterial in an animal model. Currently, there is limited evidence that $Ti_3C_2T_x$ nanosheets are harmful to humans. Wen et al. elucidated reproductive toxicology and neurotoxicity of $Ti_3C_2T_x$ exposure via intravenous injection and highlighted the possible adverse consequences on early pregnancy [58]. During early pregnancy, $Ti_3C_2T_x$ nanosheets accumulate in the uterus and placenta of pregnant mice and exhibit clear neurotoxic effects on the offspring. However, no effects on the reproductive ability of the female mice were observed. These findings highlight the importance of assessing both immediate and long-term effects of MXene exposure on pregnancy and offspring development. However, there are only few reports are published on this, so it is difficult to issue a universal statement that MXene are harmless to direct human use.

Biodegradation: The suitability of MXene in biomedical applications (e.g. tissue regeneration) and its safety can be evaluated based on its acceptable biodegradation behaviour. The hydrophilic surface of MXenes facilitates better dispersion, however, aggregation is physiological medium is a challenge. So, its biodegradation can be altered by surface modifications[59,60]. It has been shown that MXenes administrated either orally or intravenously, tend to accumulate primarily in the body organs. In toxicity management, Macrophages in the liver and spleen, particularly Kupffer cells, play an important role in their biodegradation. These cells use the human enzyme myeloperoxidase (hMPO) in the presence of hydrogen peroxide to cause oxidative degradation and facilitate the removal of MXene from the body [61]. However, the amount stored in the organs decreased over time. MXenes are broken down in the gastrointestinal tract and excreted through faeces [62]. Also, the half-lives of the different modified MXenes vary significantly. For example, the half-life of GdW10@Ti_3C_2 was 49.5 minutes[63], Nb_2C-MSNs-SNO (1.28 hrs.) [64], Ta_4C_3-SP (1.59 hrs.) [59] and Nb_2C-PVP (3.8 hrs.) [60]. Interestingly, Nb_2CT_x is currently the only one whose biodegradability has been verified [60]. In addition, organ biopsy staining following the intravenous injection of Nb_2C-PVP showed efficient metabolism of Nb_2C-PVP in all tissues. Such biodegradability of Nb_2C has facilitated its application in tissue engineering.

9. Ecological impact: A focus on the environment and human health: MXene-based adsorbents are currently being studied and have been shown to be effective in removing heavy metals from aquatic environments [65]. Nevertheless, aquatic animals and microorganisms are likely to be affected by the impulsive discharge of MXene into the environment. Considering ecological aspects, problems arise due to mass production of MXenes. Life cycle assessment (LCA) is well-known methodology that involve "cradle-to-gate" process (i.e., from raw material extraction to production) to accurately assess the potential ecological impacts associated with a particular product or process. LCA was also performed on the laboratory-scale synthesis of $Ti_3C_2T_x$ by comparing kg-$Ti_3C_2T_x$ and g-$Ti_3C_2T_x$ batches. Anasori et al. [66] found that cumulative energy demand (CED) and environmental impacts associated with kg-batches were significantly less than the other. According to LCA analysis, the ecological impacts of laboratory

production are mainly determined by energy consumption. Among the chemicals flow, titanium has harmful environmental impacts and contributes more than 70% to the overall negative impact related to material production, aluminum contributing 15%, and LiCl accounting for 10%. However, the total impact of the chemical group characterized as less than 10% of the negative effects . Therefore, to reduce the associated negative effects, the main source of $Ti_3C_2T_x$ could be recycled titanium metal for MXene production. This allows flexibility between the choice of elements and environmentally friendly metal precursors, particularly the transition metals. Electricity consumption was responsible for 70% of the negative environmental consequences of the kg-batch and 90% of g-MXene. Notably, more than 60% of the energy used in the synthesis process is attributed to high-temperature reactive sintering for MAX phase synthesis. Therefore, there is a need to develop greener and more economical synthetic processes to reduce energy consumption. However, energy consumption is strongly affected by geographical location and limitations of the laboratory. Therefore, the geographical location is important for establishing an LCA. For example, countries that rely 100% on renewable energy have the minimum environmental impact of electricity consumption.

Designing more environmentally friendly synthetic routes, at least in part, is one of the most pressing challenges in the field of MXenes. Therefore, synthesis routes must be compared in terms of their possible effects on the environment. Therefore, in an effort to evaluate the environmental performance of the synthesis pathways, different parameters such as MAX phase precursors, subsequent etching protocols, and delamination processes were involved in the LCA analysis [67]. LCA generally follows a clear pattern and suggests that HF-based approaches represent the most harmful pathway. A longer reaction time could be the reason for the potential risks associated with the direct application of HF acid, and a longer delamination time also contributed effectively. Typically, the etching process has the most significant influence on the overall environmental impact. In contrast, the synthesis approach using LiF-HCl as the etching/delamination medium is believed to have a lower environmental impact than other synthesis routes. However, the most significantly affected category was "human health", followed by "ecosystems" and "resources". Therefore, more attention needs to be paid to eco-friendly and human-friendly routes for MXene production. These investigations highlight the importance of LCA studies at laboratory-scale production. This can be useful for identifying and quantifying dominant hotspots, highlighting the need for new synthetic processes for MXenes. Moreover, understanding the MXenes LCA will be helpful for their transition from greener laboratory synthesis to industrial production.

- **Predicting the Physical properties**
- **Aqueous Stability (the so-called water attack)**
- **Surface terminations and stability**

Supplementary Information - III

10. Physical properties: Density functional theory has been widely applied to investigate the electronic and optical properties of pristine (non-terminated) and terminated MXenes [68]. Generally, pristine MXenes are expected to have a metallic nature similar to MAX phase. The electronic band structure, density of states (DOS), and partial DOS (PDOS) calculations in **Fig. S5a** indicate the metallic nature of pristine Ti_3C_2. However, depending on the terminal group, the electronic properties of MXene change from metallic to semiconducting. **Fig. S5b** shows the appearance of new bands in the energy range of −8 to −2 eV after halogen terminations (F, Cl, Br, and I) on the $Ti_3C_2X_2$ structures. In the terminated structures, Ti-d and C-p states of pristine Ti_3C_2 moved to a higher energy range. Additionally, upon termination, E_F increases (values shown in the insets), which in turn changes the bandgap and, thus, the work function (ϕ). This ultimately changes the optical properties of MXenes. This is in accordance with the work of Lau et al. [69] where the "ϕ" vary according to varying HF concentrations. This indicates that changing the type of termination or even the concentration can drastically modify the electronic and optical properties of MXenes. Readers are directed to consult ref. [70] for detailed first-principle investigation on the electronic and magnetic properties of numerous carbide and nitride MXenes with distinct functional groups.

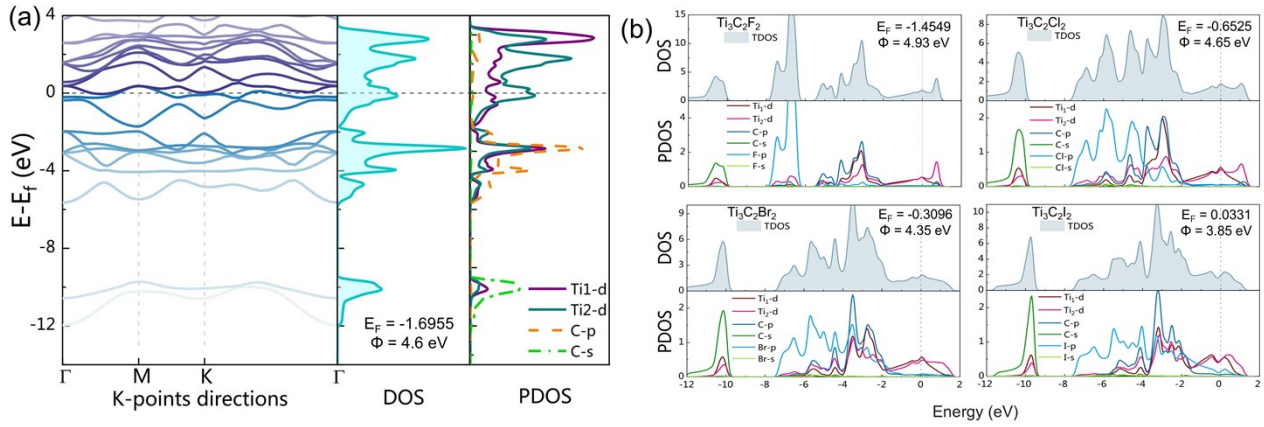

Fig. S5 (a) Electronic band structure, DOS, and PDOS distribution of pristine $Ti_3C_2T_x$. (b) DOS and PDOS distributions of halogen-terminated $Ti_3C_2T_x$. (the corresponding values of the Fermi energy and work function are also shown). *Reused after Permission from Ref. [68], copyright © 2023 Elsevier Ltd.*

11. MXenes in aqueous media: Following the previous discussion, we can assume that water plays a central role in the degradation of MXenes. This interaction between water and the MXene surface was described as "water attack". Wu et al. demonstrated this "water attack" mechanism through first-principles MD (FPMD) simulations [71]. The best way to visualise this process is to observe $(Ti\text{-}O)_{min}$, which is the closest contact between a water O-atom and surface Ti-atom. By carefully observing the water interaction through MD simulation snapshots (**Fig. S6a**) and critical distances (**Fig. S6b**), four water adsorption stages were identified. (i) Water molecules initially interact with Ti atoms on the surface, but adsorption is reversible. Water molecules come on and off, as can be seen from the oscillations in $(Ti\text{-}O)_{min}$ (ii) Irreversible chemisorption of water onto surface Ti-atoms. Water molecules pull Ti-atoms from the outer layer (indicated by an increase in the z-coordinate of Ti, $Ti_{z\text{-}max}$). This strong water-Ti interaction causes a slight surface reconstruction, resulting in irreversible adsorption. (iii) Ti atoms cause deprotonation of water, which eventually leads to the breaking of Ti–C bonds, resulting in the hydrolysis of MXenes. (iv) Finally, the newly formed –OH groups pull out Ti atoms, i.e., the formation of Ti-(OH), and the process continues (indicated by positive $Ti_{z\text{-}max}$).

According to the FPMD results, the basal planes of $Ti_3C_2O_2$ (O-terminated) are extremely susceptible to water attack by water adsorption. Therefore, to prevent MXene degradation, its reactivity with water must be reduced. Therefore, limiting the interaction of O-atoms from H_2O with the surface Ti atoms of MXene is a way to reduce water attack and therefore increase stability. For example, the hydration effect of inorganic salts in aqueous solutions can minimise the contact between MXenes and water [72]. Interestingly, experimental investigations also proved that the presence of water leads to the degradation of MXene. However, some critical issues remain unaddressed. One hypothesis is that the water attack on other Ti-atoms will probably be slowed by the protons generated during the initial attack; therefore, further research is needed to determine whether the first attack is a self-limiting process. Secondly, MXenes may contain various defects, and their reactivity with water requires further investigation. Song et al. investigated the behavior of confined water towards various defects on $Ti_3C_2O_2$ [73]. These defect regions include F-termination, O-vacancies, Ti-vacancies, and Ti-O vacancy pairs. It was shown that water molecules first interact with O-vacancies on the surface, forming –OH bonds. This negatively charged surface prevents further bonding with the surface Ti-atoms. In addition, a higher coverage of –F can prevent oxidation by limiting chemisorption on Ti-atoms. Here, it is important to emphasise that the system size and time scale obtained from the MD simulations are limited (at least in the above-mentioned studies). Another important issue to study is the interaction between bulk or unconfined water and the outer surface of MXene. However, more simulations are needed to understand these features; perhaps integration with machine learning would be beneficial.

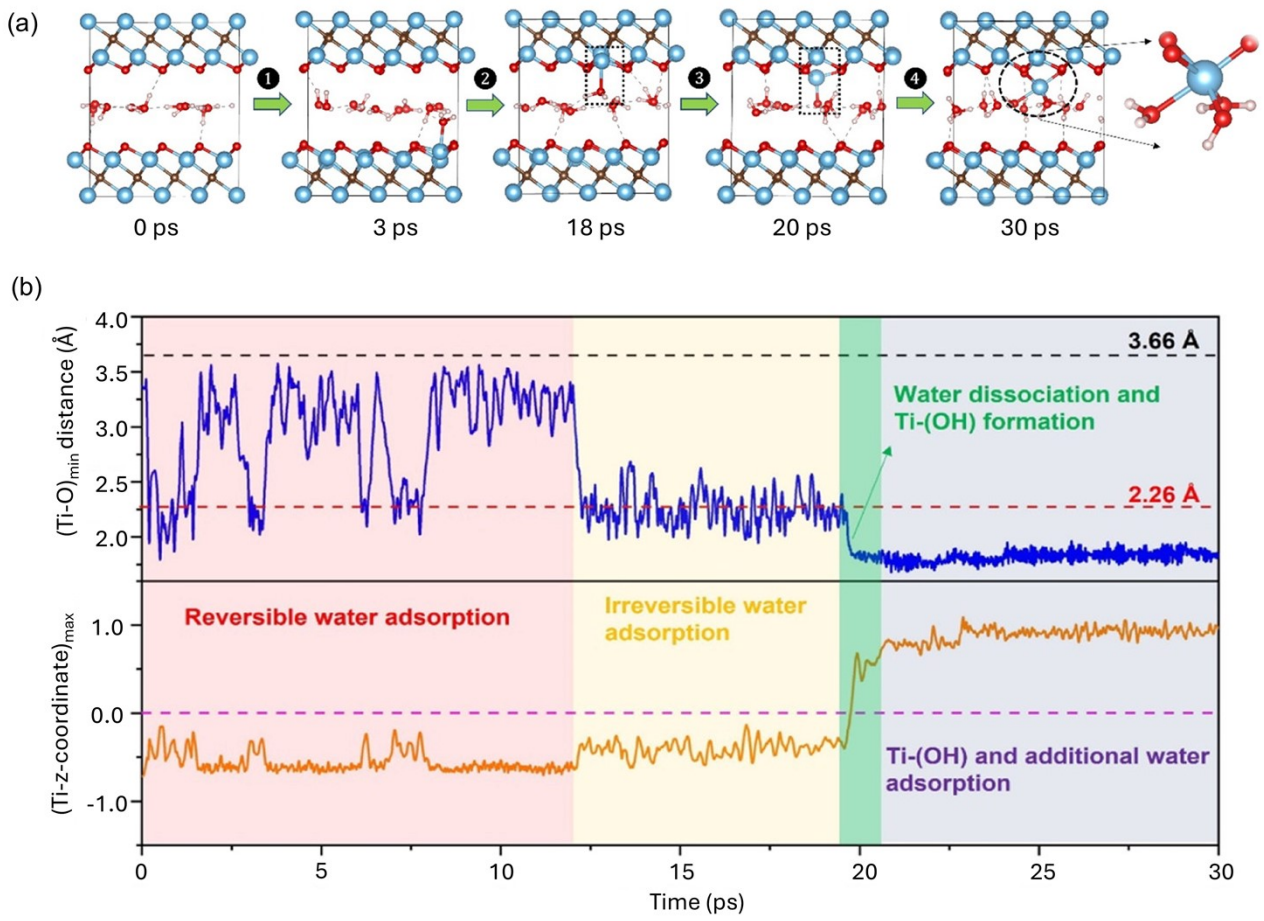

Fig. S6 (a) FPMD simulation snapshots (b) Variations in the key distance of one confined water layer with $Ti_3C_2O_2$ MXene, showing the four steps of the water attack event (simulation duration = 30 ps; T= 300 K). *Reused after Permission from Ref. [71] Copyright © 2022, American Chemical Society.*

12. On MXene's Stability: It is essential to note that during chemical etching of the MAX phases, the M-sites become highly unstable. To lower the overall Gibbs free energy of the system and reach a stable state, surface M atoms adsorb the surrounding molecules. Furthermore, MXenes possess negative formation energies, implying strong ionic/covalent bonds with termination. First-principles calculations assess the thermodynamic stabilities of MXenes by comparing the binding energies of various terminations (–O, –OH, and –F). Micheal et al. reported that $E_{exf.}$ of –O termination (~7 eV/nm^2) is greater than that of –OH and/or –F termination for both nitride and carbide counterparts [74]. Remarkably, these exfoliation energies are higher than those of graphite, which explains why intercalation and sonication are necessary to isolate MXene layers. Furthermore, smaller $E_{exf.}$ of –OH termination suggests that hydroxyl groups facilitate the isolation of the MXene layers. This is the case for intercalation with metal ions because they tend to induce more –OH groups (or water molecules) because of their hydrated state.

Rosen et al. investigated the effect of terminal groups on the physical properties and stability of several MXenes phases [75]. Besides different HF concentrations can terminate $Ti_3C_2T_x$ flakes at different rates and influence their band structure [76]. These terminal groups occupied various crystallographic positions, as shown in **Fig.S7a** (i-ii). Lau et al. considered ordered and random distributions of adatoms over the surface (**Fig**.**S7a** iii-iv) and investigated their influence on work function [69]. At all HF concentrations, the work function increased linearly with increasing –O content, whereas higher –OH concentrations showed a smaller work function (**Fig. S7b** i–iii). Furthermore, the work function increases drastically with increasing –F-terminations (increasing HF wt%). While no significant differences between the ordered and random distributions were observed. This means that the work function is independent of the distribution of adatoms (surface groups) but essentially depends on the stoichiometry (relative quantities). This also implies that the synthetic routes of MXenes can be modified to meet the requirements of specific electronic devices. Additionally, knowing the type and stoichiometry of these terminations is important for the correct interpretation of experimental results and selection of potential post-treatments.

With such an interactive surface, the stability of MXenes can be associated with the concentration of functional groups. Ternary bubble plot by Hu et al. effectively charts the role of mixed terminations (–O, –F, and –OH) on the stability of $Ti_3C_2T_x$, Ti_2CT_x, and $Nb_4C_3T_x$ MXenes (**Fig. S7-**c) [69]. Statistically, bubble size indicates the degree of stability of the respective. This intuitively provides a simpler relationship for approximating the relative stabilities at different termination ratios. Examination of the bubble plot also shows that MXenes terminated entirely in –OH are the least stable, whereas –O-terminated counterparts are the most stable. This can be attributed to our previous discussion on the stability that M atoms exist in unstable valence states (Ti^{2+} states in $Ti_3C_2T_x$ MXene) and tends to stabilise through oxidation. Because –OH is the least stable species, it is easy to desorb. Furthermore, the presence of –OH is associated with the presence of H_2O within the MXene interlayers. So, high-temperature treatment may facilitate the defunctionalization of the –OH groups. It has been experimentally shown that high-temperature annealing results in deintercalation of H_2O molecules (loss of –OH groups) and increased conductivity [6]. Furthermore, studies have reported increased stability upon scavenging ·OH radicals. Sodium bicarbonate ($NaHCO_3$) proved to be an effective ·OH scavenger and $NaHCO_3$ incorporated colloidal suspensions of $Ti_3C_2T_x$ showed increased stability up to 140 days at 5 °C and 21 days under ambient conditions [77].

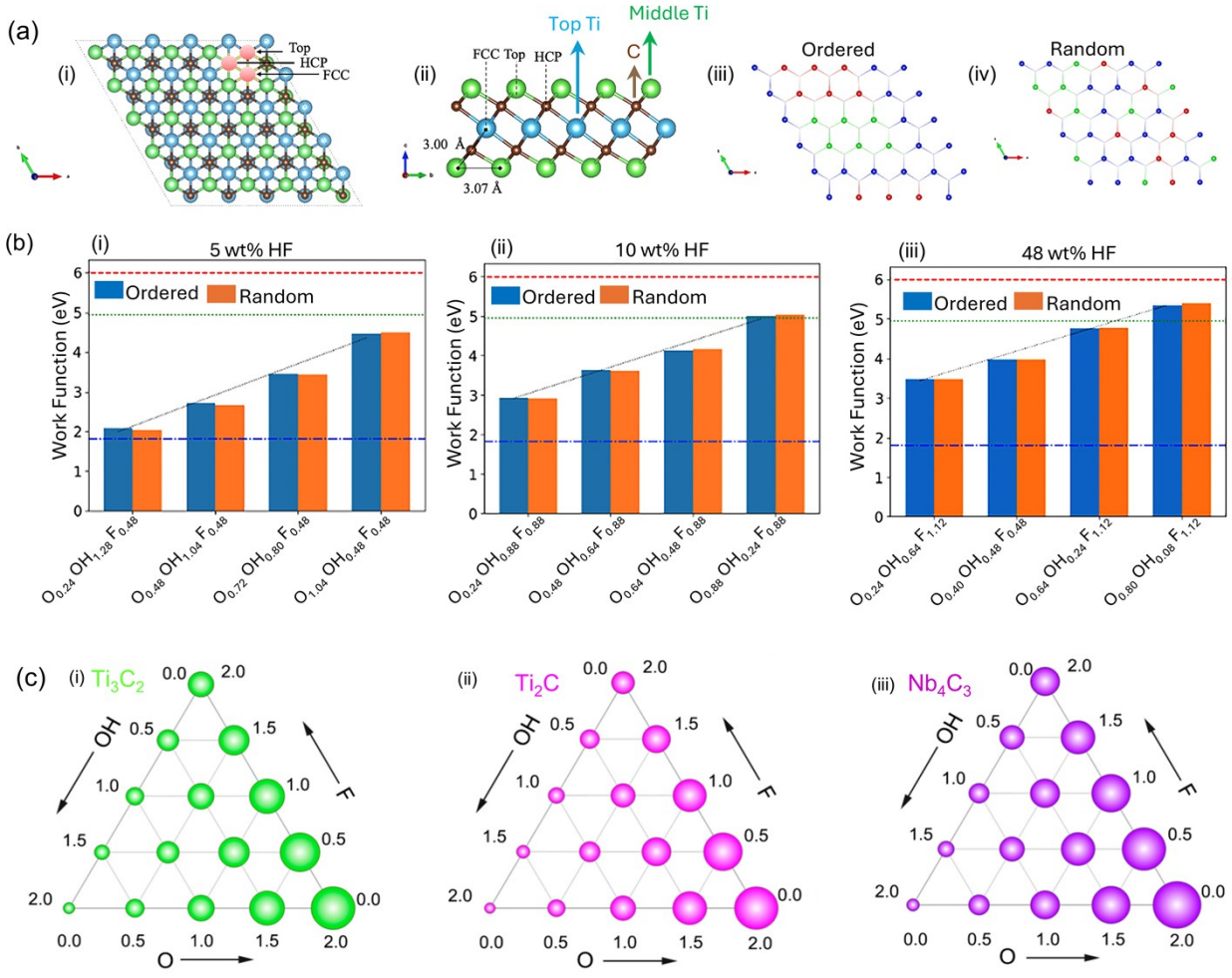

Fig. S7 (a) Atomic structure of $Ti_3C_2T_x$ MXene (i) Top-view (ii) side view (iii-iv) Illustration of ordered and random distributions of surface termination (b) Variation in work function of $Ti_3C_2T_x$ MXene at varying HF concentration (i) 5wt% (ii) (i) 10 wt% (iii) (i) 48 wt%. *Reused after Permission from Ref. [76] Copyright © 2024 The Authors. Published by Elsevier B.V.*. (c) Bubble plots of the relative stabilities of $Ti_3C_2T_x$, Ti_2CT_x, and $Nb_4C_3T_x$ at different concentrations of -O, -OH, and -F terminations. Statistically, bubble size indicates the degree of stability. *Reused after Permission from Ref. [69], Copyright © 2018 American Chemical Society.*

Supplementary Information - IV

- **Integration of DFT and Statistical Learning Models**
- **Cytotoxicity analysis of MXenes through ML**
- **Integration of MXenes with Internet of things (IoT) and 5G Technology**

13. DFT and Statistical Learning Models: It is well known that the bandgap of MXenes varies significantly with their surface terminal groups, making experimental determination of their electronic properties cumbersome. Advanced computational approaches use density functional theory (DFT) methods to efficiently evaluate the bandgaps. However, bandgap values derived from the generalised gradient approximation (GGA), or local density approximation (LDA) are often underestimated. This underestimation can be corrected using the GW method, which employs many-body perturbation theory. However, accurate determination the MXenes band gaps remains laborious and time consuming. Recently, statistical learning has shown promise in predicting the composition and properties of different material classes. Plausible chemical sources have been used to create statistical learning models that can accurately predict the MXene bandgaps. Rajan et al. constructed a learning model by employing a dataset (X, y) to map the input feature set X onto the desired GW bandgap y (**Fig. S8**) [78]. A comprehensive dataset of 23,870 MXenes was established, and a subset of 7200 MXenes was selected to provide a database with optimised structural and electronic properties. The learning models utilised input features from 76 semiconducting MXenes obtained through the DFT-Perdew–Burke–Ernzerhof functional (DFT-PBE) and the aforementioned chemical data. A metal-semiconductor categorisation model with 94% accuracy, excluding finite-gap MXenes, was then developed. This method is beneficial because of its independence from prior understanding of the PBE band gap or the conduction band maximum (CBM) and valence band maximum (VBM) positions. It can accurately estimate the GW band gaps for the entire MXene database. Moreover, evaluating and comparing various methods for predicting the material properties is crucial for developing effective prediction models. In summary, ML algorithms are crucial for the efficient synthesis of diverse 2D materials by selecting those that are most likely to be experimentally synthesised. In addition, ML, along with DFT calculations, can elucidate the synthesis principles of 2D materials by identifying critical input features for synthesizability.

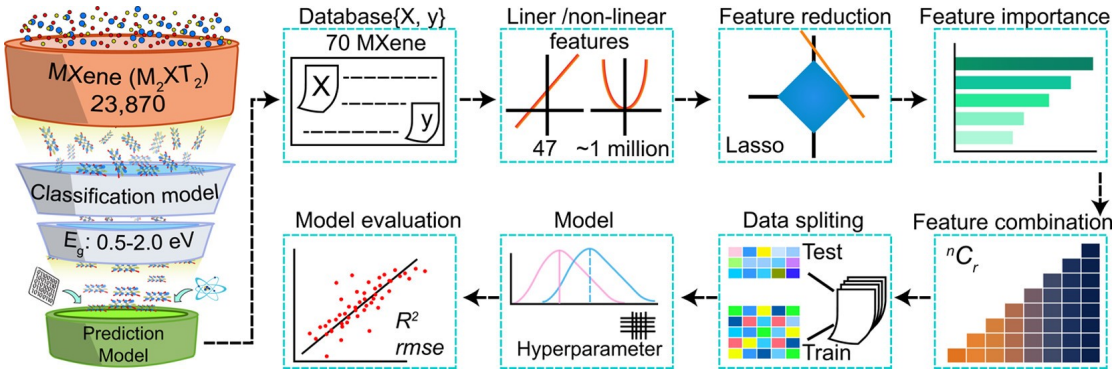

Fig. S8. Filtration of semiconducting MXenes from a known database and subsequent provision of data to the ML algorithm. During the learning process, bandgap prediction was performed using the training

dataset (X, y), where x = input features and y = output function). *Reused after Permission from Ref. [78], Copyright © 2018, American Chemical Society.*

14. Cytotoxicity: Although research on the physiological properties of MXenes and their composites is ongoing, their long-term effects remain unclear. In many cases, MXenes are transformed into bioaccessible forms using various techniques, complicating the identification of precise toxicity components and mechanisms and making reproducibility challenging. Toxicity and biodegradation are particularly concerning when MXenes and their byproducts are trapped inside tissues; poor clearance can pose health risks. A global declaration regarding the biocompatibility of MXenes is not possible owing to factors such as the synthesis process, surface groups, and flake size/shape, which can affect cytotoxicity. Each feature affects the overall toxicity, and despite formal similarities, MXenes exhibit significant property differences. Extensive research is needed in this area to address these aspects and chart a comprehensive knowledge graph. Therefore, a thorough mechanistic analysis of MXenes is necessary to accurately estimate their cytotoxicity. This is especially important as more MXenes are being used in point-of-care devices and in vivo applications. A comprehensive understanding of this process is essential for regulatory approval of MXenes for clinical use. Modelling and simulation studies may also provide insights into the potential future uses of MXenes. This suggests that research on MXenes in healthcare is still in its infancy and strict guidelines are required to guarantee their safe utilisation in biological applications. Moreover, a wide range of biological applications can benefit significantly from a wide range of MXene combinations.

15. Integration of MXenes with Internet of things (IoT) and 5G Technology

With the integration of 5G-enabled IoT devices, healthcare providers can now remotely monitor their patients in real time via continuously data streams, and diseases detection for personalised treatment. The integration of 2D materials offers numerous opportunities to improve patient outcomes and enhance the overall quality of healthcare services. The rapid advancement of smart sensor systems combining AI, ML, IoT, and 5G communication technologies are establishing a strong foundation for future research. The integration of 2D nanomaterials with the aforementioned tools is expanding sensor applications across agriculture, security, healthcare, and environmental fields [79]. In parallel, the fast transmission of data from these sensors can be ensured by the high speed and low latency 5G networks, ensuring prompt medical intervention at a distance. Such a rise of “big date in small devices” and the convergence of IoT and 5G technology has led to a range of innovative healthcare solutions, such as telemedicine. Thus, MXenes can play a crucial role in these advancements, owing to their immense potential. Tools such as radio frequency (RF) antennas are required as core components of IoT communications. Typically, metals are used for antennas, and researchers have turned nanomaterials such as graphene, carbon nanotubes, and conductive polymers into portable antennas; but their poor conductivity limits their usefulness. Studies have shown the potential of spray-coated MXenes as antennae [80] and printed MXenes as RFID tags [45]. This could meet the growing demand for thin, wearable electronic devices as IoT continues to advance. Also, integrating MXenes with IoT devices can significantly enhance the accuracy and functionality of smart implants, thereby enabling seamless real-time data transmission and personalised medical care [79,81]. Another important viewpoint is the Internet of Medical Things (IoMT), a subset of IoT technology that includes

networked medical devices used for remote patient monitoring. IoMT, also known as healthcare IoT, employs automation, sensors, and ML algorithms for health monitoring without human intervention [81]. These devices facilitate secure medical data transmission between medical professionals and patients, reducing hospital visits, acts like "Hospital on a Chip" technology. Furthermore, IoMT encompasses both point-of-care (POC) equipment in hospitals and wearable devices for real-time home health monitoring. With the advances in digital healthcare, traditional methods are being transformed through integrated cloud resources and automated tracking technologies to make high-quality healthcare more accessible, particularly in rural areas. Portable health monitoring devices, such as ultrasound machines, thermometers, and glucose meters, are increasingly common and often feature cloud storage and internet access. Moreover, a smart home medication delivery system uploads a patient's medical history to the cloud and notifies physicians if a patient misses a prescribed medication, also reminds both physicians and patients about the necessary medications [82,83]. As the population grows, technological innovations, industrial adaptation, and urbanisation place a greater demand on the healthcare system. Although MXenes show promise in healthcare applications, there are challenges for their seamless integration to current healthcare systems. Future studies should focus on biocompatibility, scalability, and data security to provide innovative and reliable healthcare solutions.

References:

(1) Maleski, K.; Ren, C. E.; Zhao, M.-Q.; Anasori, B.; Gogotsi, Y. Size-Dependent Physical and Electrochemical Properties of Two-Dimensional MXene Flakes. *ACS Applied Materials & Interfaces* **2018,** *10* (29), 24491.

(2) Shekhirev, M.; Shuck, C. E.; Sarycheva, A.; Gogotsi, Y. Characterization of MXenes at every step, from their precursors to single flakes and assembled films. *Progress in Materials Science* **2021,** *120*, 100757.

(3) Maleski, K.; Shuck, C. E.; Fafarman, A. T.; Gogotsi, Y. The Broad Chromatic Range of Two-Dimensional Transition Metal Carbides. **2021,** *9* (4), 2001563.

(4) Abdolhosseinzadeh, S.; Jiang, X.; Zhang, H.; Qiu, J.; Zhang, C. Perspectives on solution processing of two-dimensional MXenes. *Materials Today* **2021,** *48*, 214.

(5) Guo, T.; Zhou, D.; Deng, S.; Jafarpour, M.; Avaro, J.; Neels, A.; Heier, J.; Zhang, C. Rational Design of Ti3C2Tx MXene Inks for Conductive, Transparent Films. *ACS Nano* **2023,** *17* (4), 3737.

(6) Hart, J. L.; Hantanasirisakul, K.; Lang, A. C.; Anasori, B.; Pinto, D.; Pivak, Y.; van Omme, J. T.; May, S. J.; Gogotsi, Y.; Taheri, M. L. Control of MXenes' electronic properties through termination and intercalation. *Nature Communications* **2019,** *10* (1), 522.

(7) Zhang, J.; Kong, N.; Uzun, S.; Levitt, A.; Seyedin, S.; Lynch, P. A.; Qin, S.; Han, M.; Yang, W.; Liu, J.et al. Scalable Manufacturing of Free-Standing, Strong Ti3C2Tx MXene Films with Outstanding Conductivity. **2020,** *32* (23), 2001093.

(8) Alhabeb, M.; Maleski, K.; Anasori, B.; Lelyukh, P.; Clark, L.; Sin, S.; Gogotsi, Y. Guidelines for Synthesis and Processing of Two-Dimensional Titanium Carbide (Ti3C2Tx MXene). *Chemistry of Materials* **2017,** *29* (18), 7633.

(9) Shekhirev, M.; Busa, J.; Shuck, C. E.; Torres, A.; Bagheri, S.; Sinitskii, A.; Gogotsi, Y. Ultralarge Flakes of Ti3C2Tx MXene via Soft Delamination. *ACS Nano* **2022,** *16* (9), 13695.

(10) Hantanasirisakul, K.; Chantaurai, T.; Limsukhon, A.; Chomkhuntod, P.; Poprom, P.; Sawangphruk, M. Size Selection and Size-Dependent Optoelectronic and Electrochemical Properties of 2D Titanium Carbide (Ti3C2Tx) MXene. **2022,** *9* (35), 2201457.

(11) Weng, G.-M.; Mariano, M.; Lipton, J.; Taylor, A. D. In *2D Metal Carbides and Nitrides (MXenes): Structure, Properties and Applications*; Anasori, B.;Gogotsi, Y., Eds.; Springer International Publishing: Cham, 2019, DOI:10.1007/978-3-030-19026-2_12 10.1007/978-3-030-19026-2_12.

(12) Zhang, C.; Naguib, M. *Transition Metal Carbides and Nitrides (MXenes) Handbook: Synthesis, Processing, Properties and Applications*; John Wiley & Sons, 2024.

(13) Lee, A.; Shekhirev, M.; Anayee, M.; Gogotsi, Y. Multi-year study of environmental stability of Ti3C2Tx MXene films. *Graphene and 2D Materials* **2024**, DOI:10.1007/s41127-024-00076-8 10.1007/s41127-024-00076-8.

(14) Chae, Y.; Kim, S. J.; Cho, S.-Y.; Choi, J.; Maleski, K.; Lee, B.-J.; Jung, H.-T.; Gogotsi, Y.; Lee, Y.; Ahn, C. W. An investigation into the factors governing the oxidation of two-dimensional Ti3C2 MXene. *Nanoscale* **2019,** *11* (17), 8387.

(15) Cao, F.; Zhang, Y.; Wang, H.; Khan, K.; Tareen, A. K.; Qian, W.; Zhang, H.; Ågren, H. Recent Advances in Oxidation Stable Chemistry of 2D MXenes. **2022,** *34* (13), 2107554.

(16) Soomro, R. A.; Zhang, P.; Fan, B.; Wei, Y.; Xu, B. Progression in the Oxidation Stability of MXenes. *Nano-Micro Letters* **2023,** *15* (1), 108.

(17) Zhang, C. J.; Pinilla, S.; McEvoy, N.; Cullen, C. P.; Anasori, B.; Long, E.; Park, S.-H.; Seral-Ascaso, A.; Shmeliov, A.; Krishnan, D.et al. Oxidation Stability of Colloidal Two-Dimensional Titanium Carbides (MXenes). *Chemistry of Materials* **2017,** *29* (11), 4848.

(18) Doo, S.; Chae, A.; Kim, D.; Oh, T.; Ko, T. Y.; Kim, S. J.; Koh, D.-Y.; Koo, C. M. Mechanism and Kinetics of Oxidation Reaction of Aqueous Ti3C2Tx Suspensions at Different pHs and Temperatures. *ACS Applied Materials & Interfaces* **2021,** *13* (19), 22855.

(19) Habib, T.; Zhao, X.; Shah, S. A.; Chen, Y.; Sun, W.; An, H.; Lutkenhaus, J. L.; Radovic, M.; Green, M. J. Oxidation stability of Ti3C2Tx MXene nanosheets in solvents and composite films. *npj 2D Materials and Applications* **2019,** *3* (1), 8.

(20) Sunderiya, S.; Suragtkhuu, S.; Purevdorj, S.; Ochirkhuyag, T.; Bat-Erdene, M.; Myagmarsereejid, P.; Slattery, A. D.; Bati, A. S. R.; Shapter, J. G.; Odkhuu, D.et al. Understanding the oxidation chemistry of Ti3C2Tx (MXene) sheets and their catalytic performances. *Journal of Energy Chemistry* **2024,** *88*, 437.
(21) Mathis, T. S.; Maleski, K.; Goad, A.; Sarycheva, A.; Anayee, M.; Foucher, A. C.; Hantanasirisakul, K.; Shuck, C. E.; Stach, E. A.; Gogotsi, Y. Modified MAX Phase Synthesis for Environmentally Stable and Highly Conductive Ti3C2 MXene. *ACS Nano* **2021,** *15* (4), 6420.
(22) Iqbal, A.; Hong, J.; Ko, T. Y.; Koo, C. M. Improving oxidation stability of 2D MXenes: synthesis, storage media, and conditions. *Nano Convergence* **2021,** *8* (1), 9.
(23) Babar, Z. U. D.; Della Ventura, B.; Velotta, R.; Iannotti, V. Advances and emerging challenges in MXenes and their nanocomposites for biosensing applications. *RSC Advances* **2022,** *12* (30), 19590.
(24) VahidMohammadi, A.; Mojtabavi, M.; Caffrey, N. M.; Wanunu, M.; Beidaghi, M. Assembling 2D MXenes into Highly Stable Pseudocapacitive Electrodes with High Power and Energy Densities. **2019,** *31* (8), 1806931.
(25) Liu, N.; Li, Q.; Wan, H.; Chang, L.; Wang, H.; Fang, J.; Ding, T.; Wen, Q.; Zhou, L.; Xiao, X. High-temperature stability in air of Ti3C2Tx MXene-based composite with extracted bentonite. *Nature Communications* **2022,** *13* (1), 5551.
(26) Matthews, K.; Zhang, T.; Shuck, C. E.; VahidMohammadi, A.; Gogotsi, Y. Guidelines for Synthesis and Processing of Chemically Stable Two-Dimensional V2CTx MXene. *Chemistry of Materials* **2022,** *34* (2), 499.
(27) Zhang, S.; Huang, P.; Wang, J.; Zhuang, Z.; Zhang, Z.; Han, W.-Q. Fast and Universal Solution-Phase Flocculation Strategy for Scalable Synthesis of Various Few-Layered MXene Powders. *The Journal of Physical Chemistry Letters* **2020,** *11* (4), 1247.
(28) Yao, L.; Tian, X.; Cui, X.; Zhao, R.; Xiao, X.; Wang, Y. Partially oxidized Ti3C2Tx MXene-sensitive material-based ammonia gas sensor with high-sensing performances for room temperature application. *Journal of Materials Science: Materials in Electronics* **2021,** *32* (23), 27837.
(29) Seidi, F.; Arabi Shamsabadi, A.; Dadashi Firouzjaei, M.; Elliott, M.; Saeb, M. R.; Huang, Y.; Li, C.; Xiao, H.; Anasori, B. MXenes Antibacterial Properties and Applications: A Review and Perspective. **2023,** *19* (14), 2206716.
(30) Nguyen, P. H.; Nguyen, D. H.; Kim, D.; Kim, M. K.; Jang, J.; Sim, W. H.; Jeong, H. M.; Namkoong, G.; Jeong, M. S. Regenerating MXene by a Facile Chemical Treatment Method. *ACS Applied Materials & Interfaces* **2022,** *14* (45), 51487.
(31) Ahmed, H.; Alijani, H.; El-Ghazaly, A.; Halim, J.; Murdoch, B. J.; Ehrnst, Y.; Massahud, E.; Rezk, A. R.; Rosen, J.; Yeo, L. Y. Recovery of oxidized two-dimensional MXenes through high frequency nanoscale electromechanical vibration. *Nature Communications* **2023,** *14* (1), 3.
(32) Liu, L.; Orbay, M.; Luo, S.; Duluard, S.; Shao, H.; Harmel, J.; Rozier, P.; Taberna, P.-L.; Simon, P. Exfoliation and Delamination of Ti3C2Tx MXene Prepared via Molten Salt Etching Route. *ACS Nano* **2022,** *16* (1), 111.
(33) Ding, H.; Li, Y.; Li, M.; Chen, K.; Liang, K.; Chen, G.; Lu, J.; Palisaitis, J.; Persson, P. O. Å.; Eklund, P.et al. Chemical scissor–mediated structural editing of layered transition metal carbides. **2023,** *379* (6637), 1130.
(34) Du, Z.; Cheng, Z.; Zhao, Q.; Wang, H.; Zhu, Q.; Chen, H.; Chen, X.; Li, B.; Yang, S. J. a. p. a. Transformation and reconstruction towards two-dimensional atomic laminates. **2023**.
(35) Natu, V.; Barsoum, M. W. MXene Surface Terminations: A Perspective. *The Journal of Physical Chemistry C* **2023,** *127* (41), 20197.
(36) Hope, M. A.; Forse, A. C.; Griffith, K. J.; Lukatskaya, M. R.; Ghidiu, M.; Gogotsi, Y.; Grey, C. P. NMR reveals the surface functionalisation of Ti3C2 MXene. *Physical Chemistry Chemical Physics* **2016,** *18* (7), 5099.
(37) Sarycheva, A.; Gogotsi, Y. Raman Spectroscopy Analysis of the Structure and Surface Chemistry of Ti3C2Tx MXene. *Chemistry of Materials* **2020,** *32* (8), 3480.
(38) Hu, G.; Kang, J.; Ng, L. W. T.; Zhu, X.; Howe, R. C. T.; Jones, C. G.; Hersam, M. C.; Hasan, T. Functional inks and printing of two-dimensional materials. *Chemical Society Reviews* **2018,** *47* (9), 3265.

(39) Greaves, M.; Mende, M.; Wang, J.; Yang, W.; Barg, S. Investigating the rheology of 2D titanium carbide (MXene) dispersions for colloidal processing: Progress and challenges. *Journal of Materials Research* **2021,** *36* (22), 4578.
(40) Ahmed, A.; Sharma, S.; Adak, B.; Hossain, M. M.; LaChance, A. M.; Mukhopadhyay, S.; Sun, L. Two-dimensional MXenes: New frontier of wearable and flexible electronics. **2022,** *4* (4), e12295.
(41) Sreenilayam, S. P.; Ul Ahad, I.; Nicolosi, V.; Brabazon, D. MXene materials based printed flexible devices for healthcare, biomedical and energy storage applications. *Materials Today* **2021,** *43*, 99.
(42) Kedambaimoole, V.; Harsh, K.; Rajanna, K.; Sen, P.; Nayak, M. M.; Kumar, S. MXene wearables: properties, fabrication strategies, sensing mechanism and applications. *Materials Advances* **2022,** *3* (9), 3784.
(43) Cui, Y.; Zhu, J.; Tong, H.; Zou, R. Advanced perspectives on MXene composite nanomaterials: Types synthetic methods, thermal energy utilization and 3D-printed techniques. *iScience* **2023,** *26* (1), 105824.
(44) Zhang, C.; McKeon, L.; Kremer, M. P.; Park, S.-H.; Ronan, O.; Seral-Ascaso, A.; Barwich, S.; Coileáin, C. Ó.; McEvoy, N.; Nerl, H. C.et al. Additive-free MXene inks and direct printing of micro-supercapacitors. *Nature Communications* **2019,** *10* (1), 1795.
(45) Shao, Y.; Wei, L.; Wu, X.; Jiang, C.; Yao, Y.; Peng, B.; Chen, H.; Huangfu, J.; Ying, Y.; Zhang, C. J.et al. Room-temperature high-precision printing of flexible wireless electronics based on MXene inks. *Nature Communications* **2022,** *13* (1), 3223.
(46) Quain, E.; Mathis, T. S.; Kurra, N.; Maleski, K.; Van Aken, K. L.; Alhabeb, M.; Alshareef, H. N.; Gogotsi, Y. Direct Writing of Additive-Free MXene-in-Water Ink for Electronics and Energy Storage. **2019,** *4* (1), 1800256.
(47) Saleh, A.; Wustoni, S.; Bihar, E.; El-Demellawi, J. K.; Zhang, Y.; Hama, A.; Druet, V.; Yudhanto, A.; Lubineau, G.; Alshareef, H. N.et al. Inkjet-printed Ti3C2Tx MXene electrodes for multimodal cutaneous biosensing. *Journal of Physics: Materials* **2020,** *3* (4), 044004.
(48) Jastrzębska, A. M.; Scheibe, B.; Szuplewska, A.; Rozmysłowska-Wojciechowska, A.; Chudy, M.; Aparicio, C.; Scheibe, M.; Janica, I.; Ciesielski, A.; Otyepka, M.et al. On the rapid in situ oxidation of two-dimensional V2CTz MXene in culture cell media and their cytotoxicity. *Materials Science and Engineering: C* **2021,** *119*, 111431.
(49) Rasool, K.; Helal, M.; Ali, A.; Ren, C. E.; Gogotsi, Y.; Mahmoud, K. A. Antibacterial Activity of Ti3C2Tx MXene. *ACS Nano* **2016,** *10* (3), 3674.
(50) Pandey, R. P.; Rasheed, P. A.; Gomez, T.; Rasool, K.; Ponraj, J.; Prenger, K.; Naguib, M.; Mahmoud, K. A. Effect of Sheet Size and Atomic Structure on the Antibacterial Activity of Nb-MXene Nanosheets. *ACS Applied Nano Materials* **2020,** *3* (11), 11372.
(51) Arabi Shamsabadi, A.; Sharifian Gh, M.; Anasori, B.; Soroush, M. Antimicrobial Mode-of-Action of Colloidal Ti3C2Tx MXene Nanosheets. *ACS Sustainable Chemistry & Engineering* **2018,** *6* (12), 16586.
(52) Wu, W.; Ge, H.; Zhang, L.; Lei, X.; Yang, Y.; Fu, Y.; Feng, H. Evaluating the Cytotoxicity of Ti3C2 MXene to Neural Stem Cells. *Chemical Research in Toxicology* **2020,** *33* (12), 2953.
(53) Szuplewska, A.; Rozmysłowska-Wojciechowska, A.; Poźniak, S.; Wojciechowski, T.; Birowska, M.; Popielski, M.; Chudy, M.; Ziemkowska, W.; Chlubny, L.; Moszczyńska, D.et al. Multilayered stable 2D nano-sheets of Ti2NTx MXene: synthesis, characterization, and anticancer activity. *Journal of Nanobiotechnology* **2019,** *17* (1), 114.
(54) Jastrzębska, A. M.; Szuplewska, A.; Wojciechowski, T.; Chudy, M.; Ziemkowska, W.; Chlubny, L.; Rozmysłowska, A.; Olszyna, A. In vitro studies on cytotoxicity of delaminated Ti3C2 MXene. *Journal of Hazardous Materials* **2017,** *339*, 1.
(55) Scheibe, B.; Wychowaniec, J. K.; Scheibe, M.; Peplińska, B.; Jarek, M.; Nowaczyk, G.; Przysiecka, Ł. Cytotoxicity Assessment of Ti–Al–C Based MAX Phases and Ti3C2Tx MXenes on Human Fibroblasts and Cervical Cancer Cells. *ACS Biomaterials Science & Engineering* **2019,** *5* (12), 6557.
(56) Jastrzębska, A. M.; Szuplewska, A.; Rozmysłowska-Wojciechowska, A.; Chudy, M.; Olszyna, A.; Birowska, M.; Popielski, M.; Majewski, J. A.; Scheibe, B.; Natu, V.et al. On tuning the cytotoxicity of Ti3C2 (MXene) flakes to cancerous and benign cells by post-delamination surface modifications. *2D Materials* **2020,** *7* (2), 025018.

(57) Gao, F.; Xue, C.; Zhang, T.; Zhang, L.; Zhu, G.-Y.; Ou, C.; Zhang, Y.-Z.; Dong, X. MXene-Based Functional Platforms for Tumor Therapy. **2023,** *35* (51), 2302559.
(58) Wen, Y.; Hu, L.; Li, J.; Geng, Y.; Yang, Y.; Wang, J.; Chen, X.; Yu, L.; Tang, H.; Han, T.et al. Exposure to two-dimensional ultrathin Ti3C2 (MXene) nanosheets during early pregnancy impairs neurodevelopment of offspring in mice. *Journal of Nanobiotechnology* **2022,** *20* (1), 108.
(59) Lin, H.; Wang, Y.; Gao, S.; Chen, Y.; Shi, J. Theranostic 2D Tantalum Carbide (MXene). **2018,** *30* (4), 1703284.
(60) Lin, H.; Gao, S.; Dai, C.; Chen, Y.; Shi, J. A Two-Dimensional Biodegradable Niobium Carbide (MXene) for Photothermal Tumor Eradication in NIR-I and NIR-II Biowindows. *Journal of the American Chemical Society* **2017,** *139* (45), 16235.
(61) Cui, D.; Kong, N.; Ding, L.; Guo, Y.; Yang, W.; Yan, F. Ultrathin 2D Titanium Carbide MXene (Ti3C2Tx) Nanoflakes Activate WNT/HIF-1α-Mediated Metabolism Reprogramming for Periodontal Regeneration. **2021,** *10* (22), 2101215.
(62) Han, X.; Huang, J.; Lin, H.; Wang, Z.; Li, P.; Chen, Y. 2D Ultrathin MXene-Based Drug-Delivery Nanoplatform for Synergistic Photothermal Ablation and Chemotherapy of Cancer. **2018,** *7* (9), 1701394.
(63) Zong, L.; Wu, H.; Lin, H.; Chen, Y. A polyoxometalate-functionalized two-dimensional titanium carbide composite MXene for effective cancer theranostics. *Nano Research* **2018,** *11* (8), 4149.
(64) Yin, H.; Guan, X.; Lin, H.; Pu, Y.; Fang, Y.; Yue, W.; Zhou, B.; Wang, Q.; Chen, Y.; Xu, H. Nanomedicine-Enabled Photonic Thermogaseous Cancer Therapy. **2020,** *7* (2), 1901954.
(65) Nasrallah, G. K.; Al-Asmakh, M.; Rasool, K.; Mahmoud, K. A. Ecotoxicological assessment of Ti3C2Tx (MXene) using a zebrafish embryo model. *Environmental Science: Nano* **2018,** *5* (4), 1002.
(66) Dadashi Firouzjaei, M.; Nemani, S. K.; Sadrzadeh, M.; Wujcik, E. K.; Elliott, M.; Anasori, B. Life-Cycle Assessment of Ti3C2Tx MXene Synthesis. **2023,** *35* (31), 2300422.
(67) Ungureanu, A.; Francini, A.; Neri, P.; Girimonte, A.; Giovanardi, R.; Ferrari, A. M.; Rosa, R. Systematic Life Cycle Environmental Impact Comparison of Alternative Synthetic Strategies for Ti3C2Tx MXene. *ACS Sustainable Chemistry & Engineering* **2024,** *12* (15), 5893.
(68) Azadi, S. K.; Zeynali, M.; Asgharizadeh, S.; Fooladloo, M. A. Investigation of the optical and electronic properties of functionalized Ti3C2 Mxene with halid atoms using DFT calculation. *Materials Today Communications* **2023,** *35*, 106136.
(69) Hu, T.; Hu, M.; Gao, B.; Li, W.; Wang, X. Screening Surface Structure of MXenes by High-Throughput Computation and Vibrational Spectroscopic Confirmation. *The Journal of Physical Chemistry C* **2018,** *122* (32), 18501.
(70) Khazaei, M.; Arai, M.; Sasaki, T.; Chung, C.-Y.; Venkataramanan, N. S.; Estili, M.; Sakka, Y.; Kawazoe, Y. Novel Electronic and Magnetic Properties of Two-Dimensional Transition Metal Carbides and Nitrides. **2013,** *23* (17), 2185.
(71) Wu, T.; Kent, P. R. C.; Gogotsi, Y.; Jiang, D.-e. How Water Attacks MXene. *Chemistry of Materials* **2022,** *34* (11), 4975.
(72) Wang, X.; Wang, Z.; Qiu, J. Stabilizing MXene by Hydration Chemistry in Aqueous Solution. **2021,** *60* (51), 26587.
(73) Song, H.; Jiang, D.-e. First principles insights into stability of defected MXenes in water. *Nanoscale* **2023,** *15* (39), 16010.
(74) Ashton, M.; Mathew, K.; Hennig, R. G.; Sinnott, S. B. Predicted Surface Composition and Thermodynamic Stability of MXenes in Solution. *The Journal of Physical Chemistry C* **2016,** *120* (6), 3550.
(75) Yusupov, K.; Björk, J.; Rosen, J. A systematic study of work function and electronic properties of MXenes from first principles. *Nanoscale Advances* **2023,** *5* (15), 3976.
(76) Chu, Y. Z.; Hoover, M.; Ward, P.; Lau, K. C. First-principles study of MXene properties with varying hydrofluoric acid concentration. *iScience* **2024,** *27* (2).
(77) Wang, J.; Xie, G.; Yu, C.; Peng, L.; Zhu, Y.; Xie, X.; Zhang, N. Stabilizing Ti3C2Tx in a Water Medium under Multiple Environmental Conditions by Scavenging Oxidative Free Radicals. *Chemistry of Materials* **2022,** *34* (21), 9517.

(78) Rajan, A. C.; Mishra, A.; Satsangi, S.; Vaish, R.; Mizuseki, H.; Lee, K.-R.; Singh, A. K. Machine-Learning-Assisted Accurate Band Gap Predictions of Functionalized MXene. *Chemistry of Materials* **2018,** *30* (12), 4031.
(79) Chaudhary, V.; Kaushik, A.; Furukawa, H.; Khosla, A. J. E. S. P. Towards 5th generation ai and iot driven sustainable intelligent sensors based on 2d mxenes and borophene. **2022,** *1* (1), 013601.
(80) Sarycheva, A.; Polemi, A.; Liu, Y.; Dandekar, K.; Anasori, B.; Gogotsi, Y. 2D titanium carbide (MXene) for wireless communication. **2018,** *4* (9), eaau0920.
(81) Chaudhary, V.; Khanna, V.; Ahmed Awan, H. T.; Singh, K.; Khalid, M.; Mishra, Y. K.; Bhansali, S.; Li, C.-Z.; Kaushik, A. Towards hospital-on-chip supported by 2D MXenes-based 5th generation intelligent biosensors. *Biosensors and Bioelectronics* **2023,** *220*, 114847.
(82) Abdul Minaam, D. S.; Abd-Elfattah, M. Smart drugs:Improving healthcare using Smart Pill Box for Medicine Reminder and Monitoring System. *Future Computing and Informatics Journal* **2018,** *3* (2), 443.
(83) AlDuaij, N. mPillBox: An open framework for a smarter pillbox. *Journal of Network and Computer Applications* **2024,** *223*, 103824.